Eur. Phys. J. D **24**, 245–248 (2003)
DOI: 10.1140/epjd/e2003-00151-4

THE EUROPEAN PHYSICAL JOURNAL D

Study of $(Al_2O_3)_n(O_x)$ clusters with $n \leq 16$ and $x = 0, 1, 2$ from first principles calculations

E.M. Fernández[1,a], G. Borstel[2], J.M. Soler[3], and L.C. Balbás[1]

[1] Dpto. de Física Teórica, Universidad de Valladolid, 47011 Valladolid, Spain
[2] Fachbereich Physik, Universität Osnabrück, 49069 Osnabrück, Germany
[3] Dpto. de Física de la Materia Condensada, C-III, Universidad Autónoma de Madrid, 28049 Madrid, Spain

Received 10 September 2002
Published online 3 July 2003 –

Abstract. The ionic and electronic structure of $(Al_2O_3)_n(O_x)$ clusters with $n \leq 16$ and $x = 0$, 1, 2 is studied by means of first principles density functional calculations, norm-conserving pseudopotentials and a numerical atomic basis set. The equilibrium geometries have been determined by total energy minimization, starting with several initial geometries for each cluster size. The trends obtained for the atomic arrangements (structural isomers, coordination numbers, "disordered" *versus* "ordered" structures, etc.) and the electronic properties (binding energies, Homo-Lumo gap and dipole moments) are discussed. For most of the oxidized clusters studied here we find that the Homo-Lumo gap and the magnitude of dipole moment of isomeric species can vary drastically.

PACS. 36.40.-c Atomic and molecular clusters – 36.40.Cg Electronic and magnetic properties of clusters – 36.40.Jn Reactivity of clusters – 61.46.+w Nanoscale materials: clusters, nanoparticles, nanotubes, and nanocrystals

1 Introduction

Aluminum oxide (alumina, Al_2O_3) in its various allotropical forms play a vital role in an increasingly large number of industrial applications: heterogeneous catalysis, thermal barriers, corrosion protection, and metal processing are but a few representative examples. Amorphous alumina is present at most crystal alumina polymorphs and at the surface of aluminium in contact to air but the understanding of the detailed mechanism of the oxidation and passivation process is still lacking. The alumina amorphous state have been related directly to γ-alumina [1], and also molten alumina is recognized as one of the precursors of the allotropic form γ-Al_2O_3 [2]. Reactions of halomethanes with γ-alumina particles from rocket exhaust has been implicated in stratospheric ozone depletion [3]. Simulations of the hydrated α-alumina (0001) surface have been performed considering both the bare surface [4] and small isolated clusters modelling that surface [5]. The results show large differences in the calculated energetics and local structural relaxations. There are numerous recent calculations of the (0001) surface of α-alumina [6–9] and of the κ-Al_2O_3 (001) and $(00\bar{1})$ surfaces [10] revealing strongly relaxed surface Al ions, which explain the abnormally-coordinated Al ions observed in bulk porous aluminas [11]. The reactivity of different non-conventional alumina surfaces to typical contaminants and radicals is largely unknown.

As a preliminary attempt to understand those process, we calculate in this paper the atomic and electronic structure of fully relaxed alumina clusters $(Al_2O_3)_n(O_x)$ with the bulk Al_2O_3 stoichiometry ($x = 0$) and with an added oxygen atom ($x = 1$) or molecule ($x = 2$). The sizes $1 \leq n \leq 16$ for stoichiometric clusters and $1 \leq n \leq 10$ for oxidised clusters are considered, resulting in a variety of "surfaces" and atomic coordinations for both, Al and O atoms. In a previous paper we have presented preliminary results for a smaller range of sizes [12]. Here we pay special attention to important electronic and geometric differences between isomeric species of some clusters. In particular, we point to the large Homo-Lumo gap variation obtained for isomers of some cluster sizes, which could have experimental relevance [13,14]. A quantitative way to discriminate the geometry of these isomers for their utilization in different applications is the chirality index recently introduced by Garzón and coworkers [15].

In Section 2 a brief description of the method of calculation, as well as a first test case study of the smaller clusters, is given. In Section 3 the results are presented and discussed and in Section 4 we present some conclusions.

2 Method of calculation and first test case

We use the first-principles density functional theory (DFT) in the local density approximation (LDA) [16]. The electronic structure code SIESTA [17] is used to solve the

[a] e-mail: eva@lcb.fam.cie.uva.es

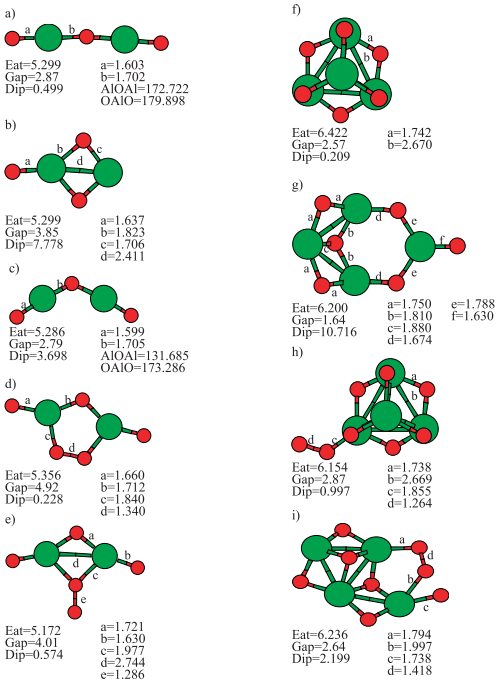

Fig. 1. Optimized geometries of the lower energy isomers of Al_2O_3 (a, b, c), $(Al_2O_3)O_2$ (d, e), $(Al_2O_3)_2$ (f, g), and $(Al_2O_3)_2O_2$ (h, i). Small spheres stand for oxygen atoms. Distances are given in angstrom (Å). Some Al-O-Al and O-Al-O angles are given. The atomization energy in eV/atom, Homo-Lumo gap in eV, and magnitude of dipole moment in Debye, are given for each aggregate.

Kohn-Sham equations using norm-conserving pseudopotentials [18] and a basis set of numerical pseudo-atomic orbitals of finite range [19]. The equilibrium geometries are relaxed by the conjugate gradient method until a maximum force smaller than 0.04 eV/Å is reached. Several initial geometries, ordered and disordered, are chosen for each cluster of the bulk stoichiometry. For $(Al_2O_3)_nO_x$ clusters, we start with several $(Al_2O_3)_n$ isomers and add an oxygen atom or molecule at different positions. For the $(Al_2O_3)_nO_2$ cases we also consider the addition of an oxygen atom to several initial $(Al_2O_3)_nO$ relaxed isomeric clusters. Then we allow the full relaxation of all the atoms. To compare with other authors, we have also optimised the position of the adsorbed oxygen atoms with the substrate cluster maintained at constant geometry. We found that such strategy may lead to results dramatically different from the fully relaxed ones.

As a first test, we have calculated the atomic structure and the electronic energy, Homo-Lumo gap, and electric dipole of $(Al_2O_3)_nO_x$ clusters with $n = 1, 2$ and $x = 0, 2$, see Figure 1. The atomisation energy is calculated as $E_{at} = -E[(Al_2O_3)_nO_x] + 2nE[Al] + (3n+x)E[O]$, where $E[Al]$ and $E[O]$ are the pseudo-atomic energies of O and Al for the free, spherical, non-spin-polarized atoms. A spin-polarized calculation of Al_2O_3 lead to the same spin-singlet minimum energy structure shown in Figure 1a. All-electron calculations at the RHF + MP2 level [21,22] have found that the lowest energy structure on the singlet potential surface is the linear D_∞ species with an Al-O (external) distance of 1.626 Å and an atomisation energy of 3.92 eV/atom More recent calculations [23] find that the C_{2v} (rhombus) structure is also a very close true minimum which fit the experiments [23]. Another calculated isomer [22] (see also Tab. I in Ref. [23]) is the V-shaped structure with C_{2v}. Our calculated isomeric geometries (a), (b), (c) in Figure 1 are similar to those obtained from RHF + MP2 calculations [23] but with shorter interatomic distances and larger atomization energies. For the O_2 molecule we obtain a bond length of 1.22 Å and a binding energy of 7.5 eV, to be compared with the experimental values 1.21 Å and 5.08 eV respectively. The generalized gradient approximation (GGA) [24] generally improves the LDA electronic energies, but not for α-$Al_2O_3(0001)$ surface [25]. However, the GGA and LDA equilibrium geometries and the relative energies between isomers, which is our main interest, are usually the same. Therefore we have consistently used the LDA in this work.

We observe in Figure 1 the sensitivity of the Homo-Lumo gap and the magnitude of electric dipole moment to different isomeric configurations. By adding an O_2 molecule to whichever of the (a), (b), (c) isomers in Figure 1, and others, at different initial sites and orientations, we obtain, after relaxing, the lowest energy equilibrium planar configuration for the Al_2O_5 cluster given in Figure 1d. Within the maximum force tolerance (0.04 eV/Å), many other equilibrium geometries are obtained with energy differences in the range of 0.2 eV/atom, *e.g.* the non-planar cluster represented in Figure 1e. As a rule of thumb, larger atomization energies correspond to larger Homo-Lumo gap and to smaller magnitude of dipole moment.

Figure 1f shows the lowest energy isomer obtained for $(Al_2O_3)_2$. The Al atoms form a tetrahedron and the O atoms cap the edges. This structure differs from the one obtained from all-electron Gaussian-94 calculations [5] by a constrained optimization. Another equilibrium geometry with 0.222 eV/atom lower atomization energy is depicted in Figure 1g. It can be viewed as the union of the two Al_2O_3 isomers depicted in Figures 1a and 1b with a gain of 0.9 eV/atom after relaxation. The adsorption of an O_2 molecule at several initial positions and distances leads, after relaxation, to the lowest energy isomer $(Al_2O_3)_2O_2$ depicted in Figure 1i. This case can be viewed as the binding of O_2 to two Al atoms of isomer (g), but can also be viewed as the relaxed product of joining the structures (b) and (d) of Figure 1. Many other isomers are obtained, *e.g.* the one depicted in Figure 1h, where the O_2 molecule binds only one O atom to one of the equivalent Al atoms of case (f).

3 Results

3.1 Atomic structure

From calculations of the Al coordination numbers and interatomic distances for all the Al-O pairs in the stoichiometric $(Al_2O_3)_n$ clusters we find a clear disordered behaviour in the range up to $n = 16$. In fact our data show

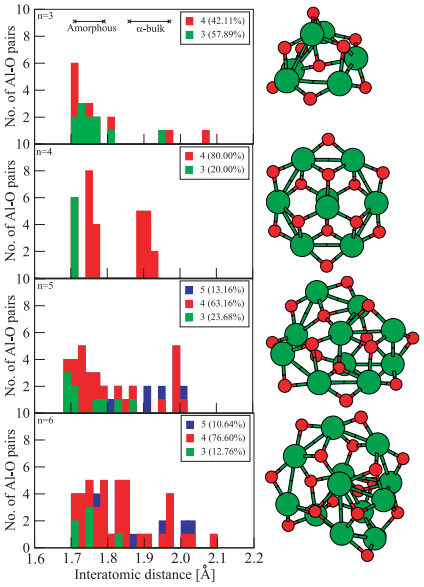

Fig. 2. Histograms of the Al-O pair distances for the lowest energy stoichiometric isomers with $n = 3$, 4, 5, 6, shown on the right. The coordination of Al atoms is indicated by different grey colours and the corresponding percentages are given for each case. The range of distances for the bulk amorphous and α phases is shown in the upper panel. Small spheres stand for oxygen atoms.

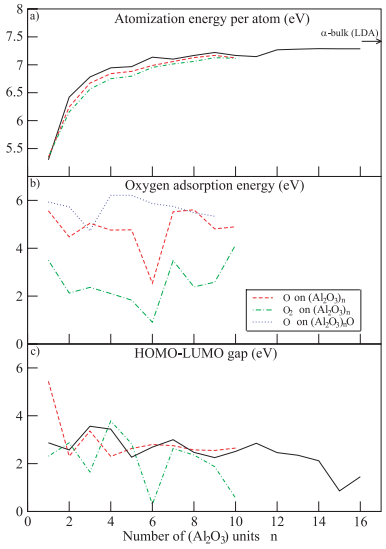

Fig. 3. Various electronic properties of $(Al_2O_3)_n(O_x)$ clusters, for fully relaxed geometries, plotted *versus* the number n of Al_2O_3 formula units. In panels (a) and (c), solid line: $x = 0$; dashed line: $x = 1$; dot-dashed line: $x = 2$. In panel (b) is given the adsorption energy of O on $x = 0$ and $x = 1$ clusters, and O_2 on $x = 0$ clusters. The arrow in panel (a) is the calculated bulk binding energy.

Table 1. The difference in atomization energy ΔE_{at} (second column, in eV/atom), the Homo-Lumo gap (third and fourth columns, in eV), and the magnitude of dipole moment (fifth and sixth columns, in Debye), for the two lower energy structures of stoichiometric $(Al_2O_3)_n$ clusters with selected values of n (first column). The asterisk (*) in columns fourth and sixth indicate the higher energy isomer.

n	ΔE_{at}	gap	gap*	dipole	dipole*
3	0.2376	3.56	0.56	0.916	8.655
4	0.0492	3.44	3.38	0.479	3.706
5	0.2556	2.27	0.72	8.177	4.976
6	0.0639	2.69	2.21	7.349	9.543
7	0.0001	3.00	3.02	8.868	1.959
12	0.0955	2.46	1.34	6.977	11.772
13	0.1790	2.35	0.45	10.189	5.882
15	0.1515	2.46	1.27	15.197	14.889

for $4 \leq n \leq 16$ the majority (60−80%) of Al atoms to be fourfold coordinated at Al-O distances typical for the amorphous phases, similar to those found in reference [1]. The radii of bond used for Al and O are 1.4 Å and 0.74 Å respectively. The number of sixfold coordinated Al atoms, which is 100% in the ordered phase, never exceeds 8% in that size range. Details of this evolution and that for the clusters $(Al_2O_3)_n(O_x)$ with $x = 1$ or 2 will be presented and discussed elsewhere. Here we show only, in Figure 2, the distribution of coordination numbers for the lowest energy isomer of $(Al_2O_3)_n$ with $n = 3$, 4, 5, and 6. Our structure for the case $n = 4$, Al_8O_{12}, is different from the one obtained in reference [5] by means of a constrained optimization using the Gaussian 94 series of programs. In the range of sizes studied in this work, the coordination of Al atoms can change drastically between isomeric configurations. For example, for an isomer of $(Al_2O_3)_4$ in Figure 2b with only 0.051 eV/atom lower atomization energy, we find Al coordinations 3 and 4 in 55.56% and 44.44% of the Al-O bonds, respectively. For most of the stoichiometric and oxidized clusters studied here, we find at least two structural isomers within an energy range typically smaller than 0.2 eV per atom showing different degrees of "order" and different electronic properties, see Table 1 and Figure 4. The two isomers of $(Al_2O_3)_7$ reported in our previous work [12], roughly correspond to the low and high density amorphous cases given in reference [1].

A major structural feature in all $(Al_2O_3)_n$ clusters studied here is the Al_2O_2 rhombus, formed between two AlO_4 units sharing two O atoms. This is a typical feature in aluminum oxide materials and is also found for small clusters [23]. A detailed analysis of these structural features will be given in a forthcoming publication.

3.2 Electronic properties

In Figure 3 several electronic properties of $(Al_2O_3)_n(O)_x$ clusters are shown. In panel (a) we see the convergence of the binding energy per atom of $(Al_2O_3)_n$ clusters towards the calculated LDA value of the bulk α-phase [6], which is already almost reached for $n = 16$. We note some extra stability for the case $n = 6$. In panel (b) adsorption energies of atomic and molecular oxygen are shown for the fully relaxed configurations. Keeping the geometry of the $(Al_2O_3)_n$ part fixed can result in unphysical values of the adsorption energies and a dissociation of the O_2 part [12]. We see in Figure 3b that the adsorption energy of an O atom on $(Al_2O_3)_n$ and on $(Al_2O_3)_nO$ clusters is roughly the same, in the range of ~ 5−6 eV, whereas the adsorption energy of an O_2 molecule on $(Al_2O_3)_n$ is in the range of ~ 2−4 eV. The exception is the case $n = 6$. Figure 2c shows the Homo-Lumo gap for all the fully relaxed clusters calculated in this work. The gap of the $(Al_2O_3)_n$

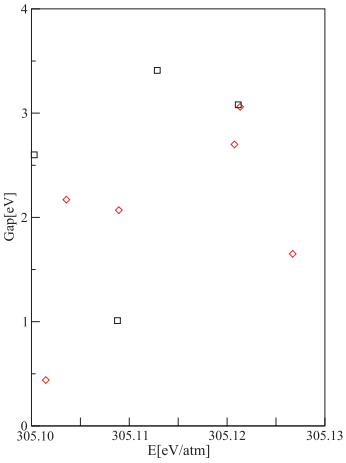

Fig. 4. The Homo-Lumo gap *versus* total energy per atom for the nine lower energy isomers of $(Al_2O_3)_3O_2$ clusters. Diamonds corresponds to relaxed geometries from initial geometries formed by adding an O_2 molecule to different positions of several initial $(Al_2O_3)_3$ isomers. The squares denote isomers optimized from adding an O atom to different $(Al_2O_3)_3O$ isomers.

clusters is reduced in several cases by the effect of O_2 adsorption. A similar result has been obtained recently for silicon nanoclusters [26]. On the other hand, the change of the Homo-Lumo gap for different isomers of selected clusters is illustrated in Table 1 and Figure 4.

In Table 1 we give the energy difference for the two lower energy structures of selected stoichiometric clusters, and the corresponding Homo-Lumo gap and magnitude of the electric dipole moments. An index to classify the "disorder" of structures, like the chirality index [15], should be of help to study the relations between structural and electronic properties of these isomers.

In Figure 4 we show the Homo-Lumo gap for the nine lower energy isomers of $(Al_2O_3)_3O_2$ within a range of 0.03 eV/atom. Isomers denoted with diamonds are obtained after relaxing initial geometries formed by adding an O_2 molecule at different positions of several $(Al_2O_3)_3$ isomers. The isomers denoted with squares result from relaxing initial geometries formed by adding an O atom to different $(Al_2O_3)_3O$ isomers. In the first case, the relaxed geometries show an O_2 group whereas in the second case any O_2 group is found generally in the relaxed structure, and one of the O atoms is bound to only one of the Al atoms. An exception is the structure with a Homo-Lumo gap $\sim$ 3 eV in Figure 4, where the second optimization route leads to the same geometry than the first route, that is, with an O_2 group. Similar results as those depicted in Figure 4 are obtained for mostly of the oxidized clusters calculated in this work.

4 Conclusions

The atomic and electronic structures of $(Al_2O_3)_n(O)_x$ clusters with $n \leq 16$ and $x = 0$, 1, 2 are obtained from first principles self-consistent LDA calculations. The Al-O interatomic distances and Al coordination numbers of the stoichiometric $(Al_2O_3)_n$ clusters display values in the range of those corresponding to the amorphous phase and the different allotropic forms of bulk alumina. Structural isomers showing amorphous-like or more ordered atomic configurations are found within a few meV/atom energy difference, particularly for O_2 oxidized clusters. The properties of clusters with an oxygen atom or molecule adsorbed on $(Al_2O_3)_n$ or $(Al_2O_3)_nO$, considered as alumina surface models, show a high degree of relaxation with pronounced effects on the electronic structure. In some cases, the Homo-Lumo gap of the oxidized clusters is reduced dramatically with respect to the stoichiometric ones.

A large number of isomers is found for the oxidized clusters, with an enormous variation in their structural and electronic properties. This fact should be taken into account by the experimentalists when interpreting their results about properties of clusters deposited on surfaces.

EMF and LCB appreciate the support of the Junta de Castilla y León (grant VA073/02) and from the MCyT (grant PB98-0368-C02). JMSM acknowledges support from the Fundación Ramón Areces and from the MCyT (grant BFM-2000-1312). EMF acknowledges a FPU grant from MECD of Spain.

References

1. G. Gutiérrez *et al.*, Phys. Rev. B **65**, 104202 (2002)
2. S. Ansell *et al.*, Phys. Rev. Lett. **78**, 464 (1997)
3. G.N. Robinson *et al.*, J. Phys. Chem. B **101**, 4947 (1997)
4. K.C. Hass *et al.*, Science **282**, 265 (1998)
5. J.M. Wittbrodt *et al.*, J. Phys. Chem. B **102**, 6539 (1998)
6. D.J. Siegel *et al.*, Phys. Rev. B **65**, 085415 (2002)
7. X.-G. Wang *et al.*, Phys. Rev. Lett. **84**, 3650 (2000)
8. I. Batyrev *et al.*, Faraday Discuss. **114**, 33 (1999)
9. E.A. Jarvis *et al.*, J. Phys. Chem. B **105**, 4045 (2001)
10. C. Ruberto *et al.*, Phys. Rev. Lett. **88**, 226101 (2002)
11. R.-S. Zhou *et al.*, Acta Cryst. B **47**, 617 (1991)
12. E.M. Fernandez *et al.*, Thin Solid Films (in press, 2003)
13. E. Heifets *et al.*, Surf. Sci. **513**, 211 (2002)
14. K.-H. Meiwes-Broer, DFG-Schwerpunktprogram 1153
15. I.L. Garzón *et al.*, Phys. Rev. B **66**, 73403 (2002)
16. J. Perdew, A. Zunger, Phys. Rev. B **23**, 5048 (1981)
17. J.M. Soler *et al.*, J. Phys. Cond. Matt. **14**, 2745 (2002)
18. N. Troullier, J.L. Martins, Phys. Rev. B **43**, 1993 (1991)
19. We use a core radius 1.14 Bohr for $2s$, $2p$, $3d$, and $4f$ states of atomic oxygen (with $2s^2 2p^4$ valence electrons), and 2.28 Bohr for $3s$, $3p$, $3d$, and $4f$ states of atomic aluminium (with $3s^2 3p^1$ valence electrons). For Al we include non-linear core corrections [20] with a core correction radius of 1.5 Bohr. We use a double zeta plus polarization (DZP) basis, with double s-p orbitals and single d polarization orbitals. Their maximum cut-off radii are 3.94 Å for O and 7.10 Å for Al. The matrix elements of the selfconsistent potential are evaluated by integration in a uniform mesh with an equivalent plane wave cut-off of 120 Ry
20. S.G. Louie *et al.*, Phys. Rev. **26**, 1738 (1982)
21. A.V. Nemukin *et al.*, J. Chem. Phys. **97**, 3420 (1992)
22. V.G. Solomonik, V.V. Sliznev, Russ. J. Inorg. Chem. **32**, 788 (1987)
23. S.R. Desai *et al.*, J. Chem. Phys. **106**, 1309 (1997)
24. J. Perdew *et al.*, Phys. Rev. Lett. **77**, 3856 (1996)
25. A.E. Mattsson, D.R. Jennison, Surf. Sci. Lett. **520**, 611 (2002)
26. A. Puzder *et al.*, Phys. Rev. Lett. **88**, 097401 (2002)